RETRIEVE GROUND PARAMETERS FROM QUASI-COHERENT TARGETS FOR SAR INTERFEROMETRY

Li Tao [(1), (2)], Hong Zhang [(1)*], Chao Wang [(1)], Yixian Tang [(1)], Fan Wu[(1)], Bo Zhang[(1)]

[(1)] Center for Earth Observation and Digital Earth, CAS, *No. 9 Dengzhuangnan Road, Haidian District, Beijing, 100094, China*
[(2)] *Graduate University of Chinese Academy of Sciences, Beijing, 19 A Yu Quan Road, Beijing, 100049, China*
Email: hzhang@ceode.ac.cn

ABSTRACT

This paper presents a multi-baseline DInSAR algorithm to obtain ground deformation and topography parameters from Quasi Coherent Targets (Q-CTs), such as the bare land and light cultivated areas that distribute broadly on the suburban ground surface. In this study the physical classification characteristics and coherence features are analyzed for Q-CTs targets selection. And a linked parameters model is established to retrieve the ground geometric information by temporally analyzing the whole stack SAR images. The ALOS PALSAR dataset over Tianjin, China is collected for the algorithm experiment. The experiment results are consistent with the levelling measurement and the investigation. Meanwhile, the estimated topography is also validated by the SRTM DEM data. The Q-CTs DInSAR algorithm brings practical applications for large scale non-urban areas monitoring.

1. INTRODUCTION

Multi-baseline Differential Synthetic Aperture Radar Interferometry (DInSAR) can retrieve long temporal surface deformation with high accuracy by stack analysis of SAR images [1, 5, 7, 8]. Generally it's accomplished by stable Coherent Targets (CTs) selection and coherent phase information processing, such as the well known Permanent Scatterer InSAR (PS-InSAR) technique [1], the Small-Baseline Subset (SBAS) algorithm [7], and the Coherent Pixels Technique (CPT) [5]. Besides the deformation monitoring, the elevation measurements based on CTs have also been studied in some literatures [3, 6].

In recent years, more industrial factories have moved to the suburban areas and led to the happening of ground subsidence. On the other hand, the monitoring means have not been established yet in time for the vast regions. Therefore, the deformation monitoring based on SAR technique can be an efficient tool. However, the main drawback of CTs related InSAR techniques is the low spatial density of detectable CTs in the vegetated non-urban areas, which may prevent from monitoring the area of interest. As known that, the Quasi-Coherent Targets (Q-CTs) exist broadly and densely on the suburban ground surface, such as the bare soil, the ground, and the light vegetation areas. With uniform scattering properties in the SAR resolution, though not strong as the CTs, these targets still can be coherently observed in SAR pairs with proper baselines. Therefore, the study of Q-CTs can give effective monitoring for the suburban areas with SAR techniques. Notice that some literatures have also exploited the distributed scatterers or partially coherent targets to obtain displacement and terrain parameters in some special monitoring circumstances [2, 4], which are the different applied situations from this study.

In this paper we focus on the displacement measuring of suburban areas. As most of these regions are mixtures of various type objects, the characterization of Q-CTs needs fully exploited for targets separation and selection. Moreover, considering the space related phase errors, such as atmospheric phase screen and orbit deviation errors, a weighted network for neighbouring targets is built and a linked parameters model is established to obtain deformation pattern and topographic parameter by jointly analyzing the coherence and phase information.

15 L-band ALOS PALSAR images over Tianjin, China are gathered for the algorithm experiment. A dense ground surface deformation map is obtained, together with a topography estimation that can represent the local terrain of the scene. The experiment results show the practical application of the Q-CTs DInSAR algorithm.

2. ALGORITHM

Suppose there are M interferograms formed by N SAR images acquired at the ordered times (t_1, K, t_N), the differential interferograms set can be generated after the phase components of both flatten earth and topography are corrected. Now consider the phase variation $\delta\phi_{phase}$ between neighbouring pixels. For the sake of simplicity, a linear phase model is assumed as:

$$\delta\phi_{\mathrm{mod}el} = \frac{4\pi}{\lambda}(T_m \cdot \Delta v + \frac{B_m}{R_m \cdot \sin\theta_m} \cdot \Delta h) \qquad (1)$$

where T_m, B_m, R_m, θ_m are the time baseline, normal baseline, slant range, and incidence angle of the m^{th} interferogram, respectively. Δv and Δh are the velocity

Proc. 'Fringe 2011 Workshop', Frascati, Italy,
19–23 September 2011 (ESA SP-697, January 2012)

variation and elevation variation of two neighbouring pixels.

For the Q-CTs network built by the Delauney triangulation, the linked parameters model is established as equation (2) by exploiting both the phase and coherence information.

$$\xi = \left| \sum_{m=1}^{M} I_m \cdot \exp\{j[\delta\phi_{phase}(m) - \delta\phi_{\mathrm{mod}\,el}(m)]\} \right| / \sum_{m=1}^{M} I_m \tag{2}$$

where $I_m(p_i, p_j) = |\gamma_m(p_i) \cdot e^{j\cdot\varphi_{p_i}} + \gamma_m(p_j) \cdot e^{j\cdot\varphi_{pj}}|$ is defined as the linked coherence of the pixel pairs (p_i, p_j) on the m^{th} interferograms, which is supposed to describe the coherence properties of the network connections, $\gamma_m(p_i)$ and $\gamma_m(p_j)$ are the pixel spatial coherence of pixels (p_i, p_j), ϕ_{p_i} and ϕ_{p_j} are the pixel interferometry phases, and ξ is referred as the temporal ensemble coherence which can describe the fitting qualities of the system model.

A maximizing process can be applied to equation (2), and the unknown parameters can be estimated when the temporal ensemble coherence ξ reaches its maximum value. Note that the defined linked coherence can index phase data with different qualities in the interferograms. During the maximizing procedure, the high linked coherence gives positive contributions to the system estimations, while the targets with low coherence will give little effect on the other data. Once the system parameters (Δv , Δh) are estimated, a further integration step is carried out to obtain the obsolete values (v, h) of each pixel.

Then in the following, the phase residues are calculated by subtracting the estimated linear deformation and terrain error from the original DInSAR phase. Here we mainly consider the separation of the residual displacement phase to obtain full deformation signal. The SVD technique can then be applied to solve the N residual phases of each SAR image from the M phase residues of each interferogram. The major source of the residual phase noise is mainly due to target decorrelation and atmospheric phase. To this aim, we firstly high pass filter the residual phases along the slant-azimuth plane in such a way to remove most of the atmosphere contribution and deal only with local deformations, and then carry out a low pass filter in time domain to obtain the nonlinear displacement contributions $\mu(t_i)$ (assuming $\mu(t_1) = 0$).

Finally, the overall deformation can be calculated by combining the linear and residual nonlinear displacements by:

$$d(t_i) = t_i \cdot v + \frac{\lambda}{4\pi} \cdot \mu(t_i), \forall i = 1, \mathrm{L}, N \tag{3}$$

3. EXPERIMENT AND RESULTS

3.1. Data Preprocessing

The test area is about 21*45 km^2 (slant range-azimuth) in Baodi county, north of Tianjin, China (see Fig. 1). In recent years, the industry construction boom has risen in Baodi, with 2 provincial development zones and 16 township industrial functional areas been constructed. Consequently, the excessive groundwater consumption has resulted in a certain ground subsidence happening. And urgently monitoring is needed. A data set of 15 ALOS PALSAR images is collected for the algorithm experiment. The distributions of temporal and normal baseline spans of the interferograms are about 874 days and 2898 m, respectively (see Tab. 1).

For the test areas, the Q-CTs targets distributed broadly and densely on the scene, mixed with other ground features. The separation of Q-CTs can efficiently reduce the effects of non Q-CTs in the parameters estimation. So in the following step a Q-CTs selected method is processed to get the target candidates.

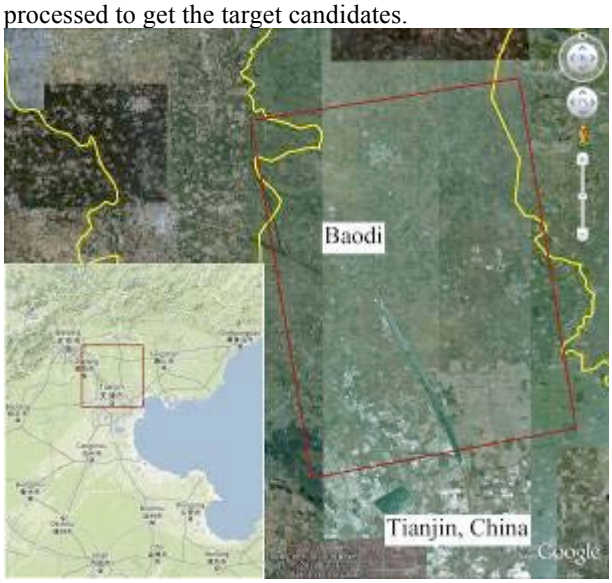

Figure 1. Test site: Suburban area of Tianjin, China. Colored frame refers to the ground coverage of the SAR data. Inset shows the location of the area of interest.

3.2. Q-CTs Candidates Selection

The *a prior* targets classifications information of the region under study can guide the separation of the Q-CTs and non Q-CTs (such as the CTs and the deccorelated targets). For SAR classification, the backscattering and texture information of each target in the SAR image is analyzed and certain algorithm is used to classify the pixels into different independent classes. In this paper we generate the classifications map based on the backscattering amplitude data. Meanwhile, the coherence information is also taken into account to select the initial Q-CTs candidates. The selection processing is implemented in the following steps:

Table 1. ALOS PALSAR data used

ID	Sensor-Scene ID	Acquisition Time	Normal Baseline (m)
1	ALPSRP130340780	2008/07/05	0
2	ALPSRP137050780	2008/08/20	-2755
3	ALPSRP143760780	2008/10/05	-1843
4	ALPSRP150470780	2008/11/20	-1542
5	ALPSRP157180780	2009/01/05	-1205
6	ALPSRP163890780	2009/02/20	-767
7	ALPSRP170600780	2009/04/07	-219
8	ALPSRP184020780	2009/07/08	-787
9	ALPSRP190730780	2009/08/23	351
10	ALPSRP197440780	2009/10/08	707
11	ALPSRP230990780	2010/05/26	1905
12	ALPSRP237700780	2010/07/11	1978
13	ALPSRP244410780	2010/08/26	2432
14	ALPSRP251120780	2010/10/11	2778
15	ALPSRP257830780	2010/11/26	2898

1) A ground targets classifications map based on the SAR amplitude images should be obtained. Note that the amplitude should be calibrated first. And the calibrated images are then averaged to get a mean amplitude map. A multi-looked operation can bring further noise elimination. After that, the ISODATA algorithm is adopted to generate the classifications map in this experiment, and seven target types are classified, such as the water bodies, the trees and dense plants, the light vegetation areas, the bare soil, the ground and road, the buildings, and the dense resident districts. We select the classes: the light vegetation areas, the bare soil, the ground and road, as the preliminary target candidates.

2) A mean coherence map should be then generated to test the phase quality of the selected candidates. The mean coherence map is formed from the whole stack of coherence maps after the generation of multilooked images. And then a threshold should be decided to accept the candidates as the checked targets set. In this study, we neglect the targets with coherence less than 0.2, which has been tested as suitable. So, by combining the two criteria, there are about 80 000 Q-CTs detected within the test area (see Fig. 2) for parameters inversion.

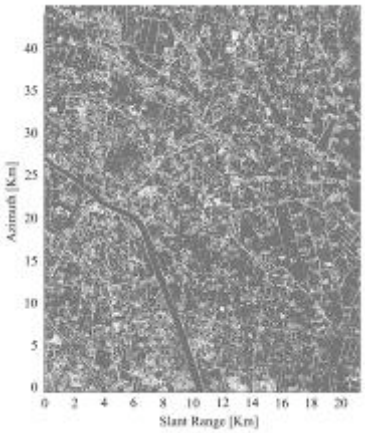

Figure 2. Selected Q-CTs candidates

3.3. Displacement and topography Measurements

We use the Q-CTs based DInSAR algorithm to obtain the displacement and terrain measurements of the study site, as shown in Fig. 3 and Fig. 4. In order to test the terrain extraction of the Q-CTs algorithm, we have processed the experiment data set without correcting its topography information. And consequently the calculated DEM error should be the true topography measurement of the scenario.

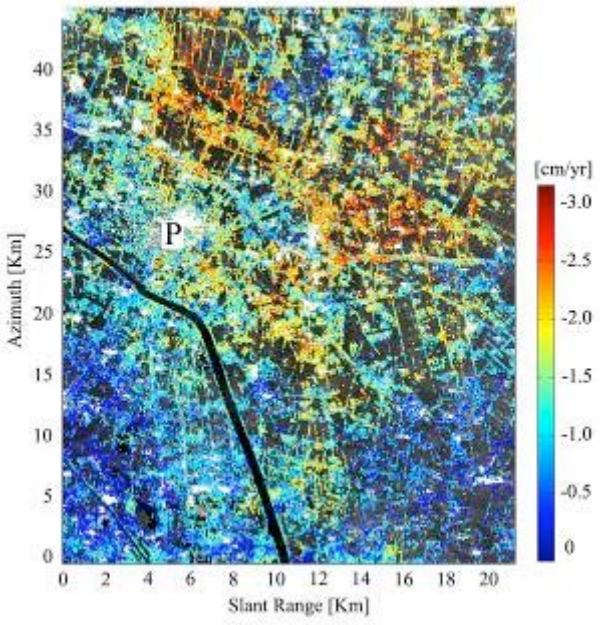

Figure 3. Deformation velocity map of the test area. The background is the mean coherence map.

Clearly as we can see in Fig. 3, the estimated ground displacements can map the vast non-urban regions with dense and detailed information. The movement has been projected onto the vertical direction. And obviously the dynamic subsidence pattern has been detected. Take the location of P (the Baodi county) as reference, three areas in the top, right, and the bottom right directions present a subsidence velocity larger than 2 cm per year during the monitoring time from 2008.07 to 2010.11.

The maximum subsidence velocity reaches 3.2cm/year. We have investigated that, corresponding to the above subsidence regions, there locate the Tianbao industry development zone, the Xin'an town and the Lintunkou town township industry functional areas, respectively. Excessive industrial groundwater consumption causes the subsidence happening in these regions. For precise data validation, the levelling measurement data over region P has been collected. In the time interval of 2008.10 to 2009.10, the levelling data gives 0.8cm of displacements whereas the corresponding SAR measurement results in 0.84cm.

Meanwhile the SRTM DEM data has been used to validate the estimated topography. Fig. 5 is the scatters plot of the InSAR height estimation and the corresponding SRTM DEM for data correlation

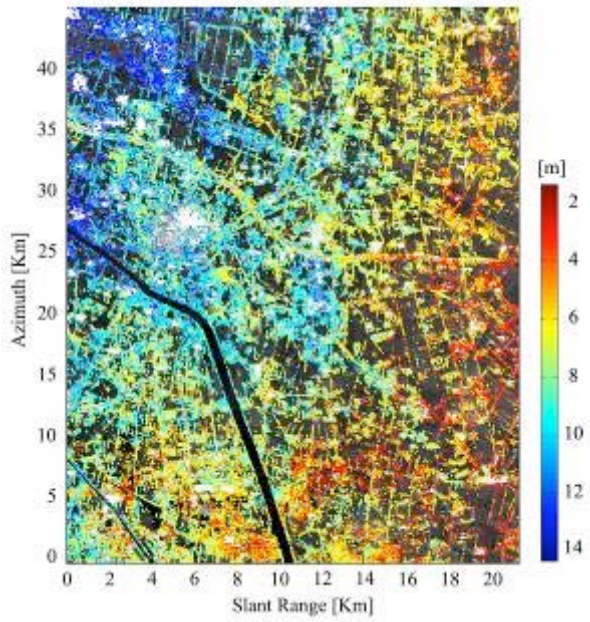

Figure 4. Estimated local topography

comparison. For the sake of brevity we average the terrain data in a 9*9 multi-looked window to get the plotted scatters in Fig. 5. It is evident the datasets are mainly gathering in the diagonal, with the data correlation of about 78%.

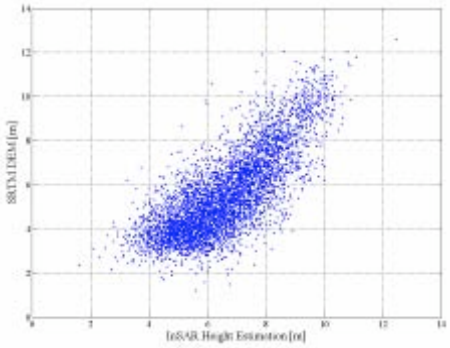

Figure 5. Scatters plot of deformation velocity between the InSAR measurement and the SRTM DEM, with the correlation of 78.46%.

4. CONCLUSIONS

This study proposes a multi-baseline InSAR method to retrieve terrain deformation and topography elevation from Quasi-Coherent Targets (Q-CTs) in the suburban areas. The complex coherence information of the Q-CTs targets has been fully exploited for model establishment and parameters retrieval. For the large-scale non-urban areas where the ground information can not be well obtained due to the lack of coherent targets, the Q-CTs InSAR analysis can retrieve precise estimations of the parameters of interest. The experiment results, by employing 15 ALOS PALSAR dataset over Tianjin, China, have shown the effectiveness of the proposed algorithm.

In the experiment both coherence and backscattering information are jointly utilized to collect target candidates. The features of Q-CTs should be in-depth explored in the further researches for more precise data estimations.

5. ACKNOWLEDGMENTS

This work is supported in part by the National Natural Science Foundation of China under Grants 40971198 and 40871191, and in part by the National High-Tech Research and Development Program of China under Grant 2011AA120404. The authors would like to thank JAXA for the ALOS PALSAR data and Tianjin Land Subsidence Controlling Office for the leveling data.

6. REFERENCES

[1] A. Ferretti, C. Prati, and F. Rocca.(2000). Nonlinear Subsidence Rate Estimation using Permanent Scatterers in Differential SAR Interferometry. *IEEE Transactions on Geoscience and Remote Sensing*, IEEE, USA, **38**(5), pp. 2202-2212.

[2] A. M. Guarnieri and S. Tebaldini.(2008). On the Exploitation of Target Statistics for SAR Interferometry Applications. *IEEE Transactions on Geoscience and Remote Sensing*, IEEE, USA, **46**(11), pp. 3436-3443.

[3] D. Perissin and F. Rocca.(2006). High-accuracy Urban DEM using Permanent Scatterers. *IEEE Transactions on Geoscience and Remote Sensing*, IEEE, USA, **44**(11), pp. 3338-3347.

[4] F. Rocca.(2007). Modeling Interferogram Stacks. *IEEE Transactions on Geoscience and Remote Sensing*, IEEE, USA, **45**(10), pp. 3289-3299.

[5] O. Mora, J.J. Mallorqui, and A. Broquetas, "Linear and Nonlinear Terrain Deformation Maps from a Reduced Set of Interferometric SAR Images", *IEEE Transaction on Geoscience and Remote Sensing*, IEEE, USA, **41**(10), pp. 2243-2253, October 2003.

[6] O. Mora, R. Arbiol, V. Pala, A.Adell, and M. Torre. (2006). Generation of Accurate DEMs using DInSAR Methodogy (TopoDInSAR)", *IEEE Geoscience and Remote Sensing Letters*, IEEE, USA, **3**(4), pp. 551-554.

[7] P. Bernardino, G. Fornaro, R. Lanari, and E. Sansosti.(2002). A New Algorithm for Surface Deformation Monitoring based on Small Baseline Differential SAR

Interferograms. *IEEE Transactions on Geoscience and Remote Sensing*, IEEE, USA, **40**(11), pp. 2375-2383.
[8] T. Wu, C. Wang, H. Zhang, Y.X. Tang, and L. Tian. (2008). Deformation Retrieval in Large Areas based on Multi-baseline DInSAR Algorithm: A Case Study in Cangzhou, Northern China. *International Journal of Remote Sensing*, Taylor & Francis, London, UK, 29(12), pp. 3633-3655.